Journal of the European Ceramic Society 22 (2002) 1205–1216
www.elsevier.com/locate/jeurceramsoc

Use of cycles of compression to characterize the behaviour of apatitic phosphate powders

C. Pontier[a,b,*], E. Champion[a], M. Viana[b], D. Chulia[b], D. Bernache-Assollant[a]

[a]*SPCTS UMR 6638, Faculté des Sciences, 123, Avenue Albert Thomas, 87060 Limoges Cedex, France*
[b]*GEFSoD EA 2631, Faculté de Pharmacie, 2, Rue du Docteur Marcland, 87025 Limoges Cedex, France*

Received 26 April 2001; received in revised form 19 August 2001; accepted 19 September 2001

Abstract

A method has been developed to analyse the bulk and mechanical properties of powders under pressure using a uniaxial press. This easy-to-use and rapid method requires small amounts of material and allows different compression parameters to be assessed. Classical parameters, e.g. compaction ratio and tensile strength, are determined. The recording of the compression and rupture cycles allows the energies of compression and of rupture to be calculated. The flowability of the powder is determined during the compression experiment. The energy of compression is linked with the elastic energy to help to explain the energy consumption during compression. It is also correlated to the rupture energy to evaluate the ability of the material to convert the energy of compaction into cohesion. This simple method has been applied to apatitic calcium phosphate powders differing in Ca/P molar ratio and/or crystallinity. It allowed to study the relation between chemical nature and compressibility. © 2002 Elsevier Science Ltd. All rights reserved.

Keywords: Apatite; Mechanical strength; Pharmaceutical applications; Pressing

1. Introduction

Hydroxyapatite (HAP) and tricalcium phosphate (TCP) powders are used in pharmaceutical industry as direct compression diluents and binders, due to their good binding and bulk properties. A regular composition, i.e. a precise and reproducible Ca/P molar ratio, is known to be difficult to obtain and control.[1] The real composition of commercial products varies between stoichiometric HAP ($Ca_{10}(PO_4)_6(OH)_2$, Ca/P = 1.667), calcium deficient HAP ($Ca_{(10-x)}(PO_4)_{(6-x)}(HPO_4)_x(OH)_{(2-x)}$, $0 < x < 1$, $1.500 < Ca/P < 1.667$), apatitic TCP ($Ca_9(PO_4)_5(HPO_4)OH$, Ca/P = 1.500), anhydrous TCP ($Ca_3(PO_4)_2$, Ca/P = 1.500) or blendings of these compounds with the possible presence of other calcium phosphates.[2] Moreover, the materials can be well-crystallised or not, depending on the elaboration process and thermal treatment. These chemical variabilities lead to confusions in the denominations and associated chemical formula of products: despite different chemical formula, the materials are sometimes supplied under the same chemical name. This is all the more troublesome that recent works have shown that very small variations of the Ca/P ratio of apatitic calcium phosphates induce great changes in the material properties. This was demonstrated for the mechanical properties and biological behavior of ceramics of interest for bone substitute applications.[3–6] Similarly, the chemical variability may induce differences in the compression properties of powders used as binders but, in this field, no results are available yet. On these bases, a rationalization of the chemistry of apatitic calcium phosphate powders used as direct compression excipients in pharmaceutical applications appears necessary.

The complete study of materials to be used in compression is usually time and material-consuming and needs to evaluate different parameters, e.g. physical properties, compaction properties, mechanical properties... The flowability is the first important parameter that governs the storage of the materials as well as the outflow of hoppers and the tablet mass uniformity. It is generally studied using the angle of repose method, flow rate or shear cells measurements.[7] The compression and the mechanical properties are classically studied using a

---

* Corresponding author at second address. Tel.: +33-5-55-43-58-53; fax: +33-5-55-43-59-10.
E-mail address: catherine-pontier@yahoo.fr (C. Pontier).

PII: S0955-2219(01)00453-8

tabletting machine and the comparison of different materials is made on the basis of the calculated porosity of the tablets and their tensile strength. These two parameters do not take into account the ability of the material to use the energy provided for the compression.

The present study is concerned with a methodology of characterization of all these parameters by compressing a small amount of material and studying its mechanical properties using an instrumented uniaxial press. It allows flowability and original compression parameters to be assessed. The behavior of well-defined apatitic calcium phosphates differing in their chemical composition or crystallinity is investigated.

2. Materials and methods

2.1. Materials

Two apatitic calcium phosphate powders with a different Ca/P molar ratio were synthesized using a classical wet method of precipitation. It consisted in the addition of a diammonium phosphate solution ($(NH_4)_2HPO_4$, Aldrich, France) into a calcium nitrate solution ($Ca(NO_3)_2$, $4H_2O$, Aldrich, France) placed in a fully automated reactor with pH and temperature regulation. The main synthesis parameters are summarized in Table 1, a more detailed description can be found elsewhere.[8] After the total addition of the reactants, the suspension was ripened for 30 min under constant stirring and temperature. Then, the precipitates were filtered under vacuum. All the precipitates were spread into a thin layer and dried ($T = 60$ °C, Memmert, Schwabach, Germany) to reach a final moisture content of 5% (w/w).

Granulation and calibration of the powders were performed without binder using an oscillating granulator with a 2 mm screen and a 315 μm screen, respectively (Erweka AR 400, Heusenstamm, Germany).

Two methods of purification were compared to eliminate synthesis residuals, i.e. ammonium nitrate. In the first one, precipitates were washed with distilled water during the filtration step. In the second one, unwashed precipitates were granulated and calibrated, then the granules were calcined for 1 h at 720 °C in air atmosphere (Kanthal Super, Rapid high temperature furnace, Bulten-Kanthal, Sweden). The four resulting batches of calibrated materials will be referred as TCPuc and HAPuc for the washed materials and TCPc and HAPc for the calcined materials.

Table 1
Synthesis conditions of the materials

Material	Ca/P molar ratio	$(Ca/P)_{reactants}$	pH	Temperature (°C)
HAP	1.667	1.667	9.5	95
TCP	1.500	1.500	7.5	40

The identification of the crystalline phases of the materials was performed using powder X-ray diffractometry (XRD). XRD patterns were recorded with CuK_α radiation on a $\theta/2\theta$ diffractometer (Siemens D5000, Germany) between 20° and 40° (2θ). The crystalline phases were deduced from a comparison of the registered patterns with the ICDD reference data file (PDF 9-432 for hydroxyapatite, PDF 9-169 for β-tricalcium phosphate, PDF 9-346 for calcium pyrophosphate and PDF 4-0777 for calcium oxide). XRD was also used to determine the Ca/P molar ratio of the powders. The samples were analysed according to an AFNOR standard specification.[9] Prior to this XRD analysis, the powders were calcined for 15 h at 1000 °C in air atmosphere, to insure a high degree of crystallinity of the powders and to insure the eventual decomposition of the calcium phosphates into two crystalline phases or less. If the Ca/P molar ratio of the material is lower than 1.667, it decomposes into β-tricalcium phosphate and hydroxyapatite, and if the Ca/P molar ratio is higher than 1.667, it decomposes into calcium oxide and hydroxyapatite. If the Ca/P molar ratio is lower than 1.5, it decomposes into β-tricalcium phosphate and calcium pyrophosphate. This method has been compared by other authors to more classical identification and quantification methods and it has been shown to be more accurate than chemical analysis (relative uncertainty on the Ca/P molar ratio: less than 0.4% for XRD versus 2.5% for chemical analysis).[10] In addition to this technique, infra-red spectroscopy was performed to be sure of the absence of other non crystalline phases.

2.2. Physical characterizations

Particle size distribution was studied by sieving, using 20 g of granules and a series of vibrating sieves from 56 to 1000 μm (Retsch AS 200 basic, Germany) according to the European Pharmacopeia procedure (2-9-12).[11] The mean diameter (D_{50}, μm) was determined for each material. A dispersion coefficient was calculated according to Eq. (1):

$$\text{dispersion coefficient} = D_{25} - D_{75} \tag{1}$$

where D_{25} is the diameter of 25% (w/w) of the retained mass of granules (μm) and D_{75} is the diameter of 75% (w/w) retained granules determined from the cumulative particle size distribution representation.

The morphology of the granulated powders has been studied using scanning electron microscopy (Hitachi S2500, Japan) after a 5 min Au/Pd metallisation.

The pycnometric density of the powders (d_{pycno}, g cm^{-3}) was determined using a helium pycnometer (Accupyc 1330, Micromeritics Instruments Inc., Norcross, GA). The samples were dried 48 h at 50 °C and the measurements were performed in triplicate.

The bulk density (d_{bulk}, g cm^{-3}) of the unpacked materials was determined by pouring 20 g of powder into a graduated cylinder and measuring its volume. d_{bulk} is calculated according to:

$$d_{\text{bulk}} = \frac{20}{V} \quad (2)$$

where M is the mass (g) of powder, and V is its volume (cm^3).

Specific surface area (Ss, m^2 g^{-1}) of the powders was measured by low temperature helium adsorption using a Gemini 2360 Analyser (Micromeritics Instruments Inc., Norcross, GA) with liquid nitrogen as a cooler. Prior to adsorption measurements, the samples were degassed for 24 h at 80 °C at a pressure lower than 4.10^{-2} Torr (VacPrep 61, Micromeritics Instruments Inc., Norcross, GA). The specific surface areas were calculated with the B.E.T. equation in the relative range of pressures of 0.05–0.30. Measurements were performed in triplicate.

Porosity measurements were performed using a mercury intrusion porosimeter (Auto-Pore III, Micromeritics Instruments Inc., Norcross, GA) using pressures from 0.0069 to 689 MPa. The samples were dried 48 hours before the measurements. The total porosity is determined as the ratio of the volume of intruded mercury and the volume of the sample. The intra-granular porosity is the ratio of the volume of mercury used to fill the intra-granular pores and the total volume of mercury. The inter-granular porosity is the ratio of the volume of mercury used to fill the inter-granular pores and the total volume of mercury.

2.3. Compression properties

The behavior of the granulated materials during compression was studied using a uniaxial press (Lloyd Instrument 6000R, Fareham, England) with a 1 cm^3 cell (height = 10 mm, surface = 10 mm^2) and flat punches. The cell was manually filled with an accurate mass of powder calculated from the bulk density of the unpacked materials (corresponding to masses between 0.2 and 0.6 g depending on the materials). The inner surface of the cell was lubricated with a thin layer of magnesium stearate before filling. Pressures from 10 up to 300 MPa were studied. The press was instrumented with an external extensometer (0–20 mm) and a force measuring sensor (0–30 000 N) to accurately measure the displacements of the upper punch during compression and breaking tests. Six compacts per pressure were manufactured.

The cycles of compression were studied as displacement versus pressure of compaction. Fig. 1 shows a characteristic compression cycle. The meaning of each part of the curve is defined hereafter.[12] The cycle corresponds to the succession of three phases. The first one is the packing of the powder without creation of bindings between the granules (OA in Fig. 1). AB in Fig. 1 corresponds to the compression itself, and BE to the unloading.

The ability of the powder to rearrange under low pressures is defined as the packing coefficient (C_T,%), calculated according to Eq. (3):

$$C_T = \frac{D_{0.5}}{H_0} \times 100 \quad (3)$$

where $D_{0.5}$ is the displacement (mm) of the upper punch for a pressure of compaction of 0.5 MPa (see Fig. 1) and H_0 is the initial height of the powder bed (10 mm).

C_T values lower than 25% characterize a good packing ability of the material, and values higher than 30% a bad packing ability.[13] The C_T values have been correlated with more classical parameters, such as the Carr coefficient. The Carr coefficient is an expression of the difference between the unpacked volume and the packed volume of powder and allows to discriminate powders according to their flowability.[14] It allowed us to obtain the same information about the flowability of a powder, using a lower amount of powder.

Different energies are calculated from the cycles of compression.

The area under the curve (ABE in Fig. 1) corresponds to the net compression work (NCW, J g^{-1}), that is the work required by the material to be compacted [Eq. (4)]. Works are normalized by dividing by the compact mass to allow a comparison between the different materials without influence of the mass.

$$NCW = \frac{\text{area ABE}}{\text{mass of the compact}} \quad (4)$$

The area BCE in Fig. 1 corresponds to the elastic work (EW, J g^{-1}) i.e. the energy associated with the expansion during unloading due to the elasticity of the compact [Eq. (5)].

$$EW = \frac{\text{area BCE}}{\text{mass of the compact}} \quad (5)$$

The EW/NCW ratio is studied to characterize the behavior of the material during compression.

The deformation mechanism was studied during compression from the Heckel plots. The Heckel equation is widely used in pharmaceutical formulation and is an expression of the porosity of the compact versus the pressure of compaction [Eq. (6)].[15]

$$-\ln\left(1 - \frac{d_{\text{compact}}}{d_{\text{pycno}}}\right) = K + bP \quad (6)$$

where d_{compact} is the apparent density of the compact (g cm^{-3}), d_{pycno} is the pycnometric density of the material

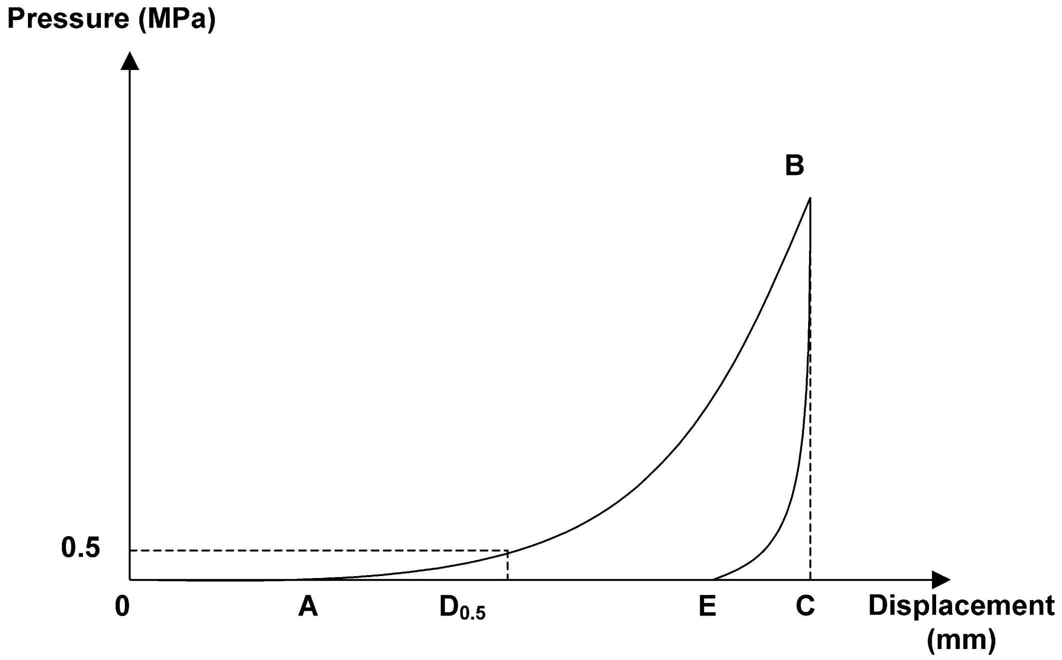

Fig. 1. Pressure versus displacement curve during a compaction test.

(g cm^{-3}), P is the compaction pressure (MPa), K and b are constants.

The mean yield pressure (Py, MPa) is determined as the reciprocal of the slope of the linear part of the Heckel curve between 70 and 150 MPa. Py values lower than 100 MPa define plastic materials, between 100 and 200 MPa intermediate materials, and higher than 200 MPa brittle materials.[15]

The compaction ratio (%) was determined, after ejection, for each compact, according to Eq. (7).

$$\text{Compaction ratio} = \frac{d_{\text{compact}}}{d_{\text{pycno}}} \times 100 \tag{7}$$

The compression range (MPa) was determined for each compound as the range of pressures allowing to obtain compacts removable from the die, without lamination.

2.4. Mechanical properties

The diametral compression test was performed, 24 h after the compaction, using 3 compacts per pressure.[16] The test was performed with the uniaxial Lloyd press to precisely measure the displacement and the applied force and to plot the cycles of rupture.

The tensile strength (R_d, MPa) was determined using Eq. 8:

$$R_d = \frac{2 \times F}{\pi \times d \times h} \tag{8}$$

where F is the maximum diametral breaking force (N), d is the diameter of the compact (mm) and h is the height (mm) of the compact after ejection.

The breaking cycles were studied during the diametral breaking tests and were plotted as force versus displacement. The general profile of a breaking cycle is shown in Fig. 2. The breaking work (BW, J g^{-1}) is calculated using Eq. (9):

$$BW = \frac{\text{area OEF}}{\text{mass of the compact}} \tag{9}$$

where OEF is the area under the cycle of rupture (Fig. 2).

3. Results and discussion

3.1. Chemical nature of the materials

XRD patterns of HAP and TCP powders calcined at 1000 °C, according to the AFNOR standard, are used to determine the Ca/P molar ratio of the materials under study. They are given in Fig. 3. They are typical of well-crystallized compounds and show that both powders are single-phased: no other diffraction peak than those corresponding either to HAP or β-TCP phase was detected on the respective patterns. IR spectra (not presented in this paper) confirmed the absence of any other vibrational band than that corresponding to the pure phase HAP or β-TCP in each powder. It can be deduced from the analysis that the HAP powders have a Ca/P molar ratio of 1.667 (−0.001, +0.005) which corresponds to stoichiometric HAP, and that the TCP powders have a Ca/P ratio of 1.500 (−0.005, +0.001) corresponding to stoichiometric TCP.[10]

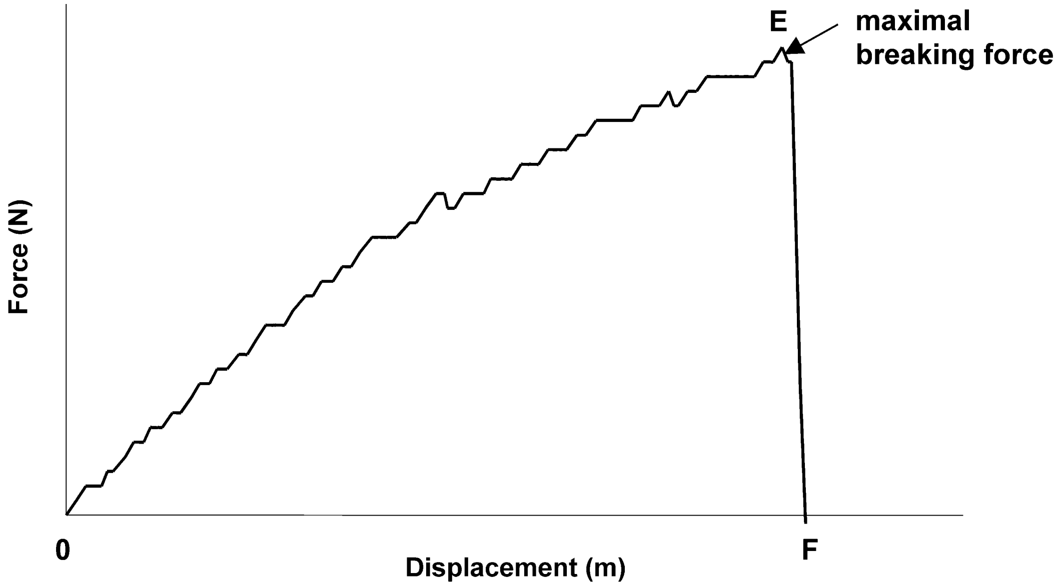

Fig. 2. General aspect of a force versus displacement curve during the diametral compressive test.

XRD patterns of HAP and TCP materials under study are given in Fig. 3a and b, respectively. They showed that all the materials are single-phased. The washed materials (HAPuc and TCPuc) exhibited an apatitic structure with broad diffraction peaks indicating a low crystallinity.

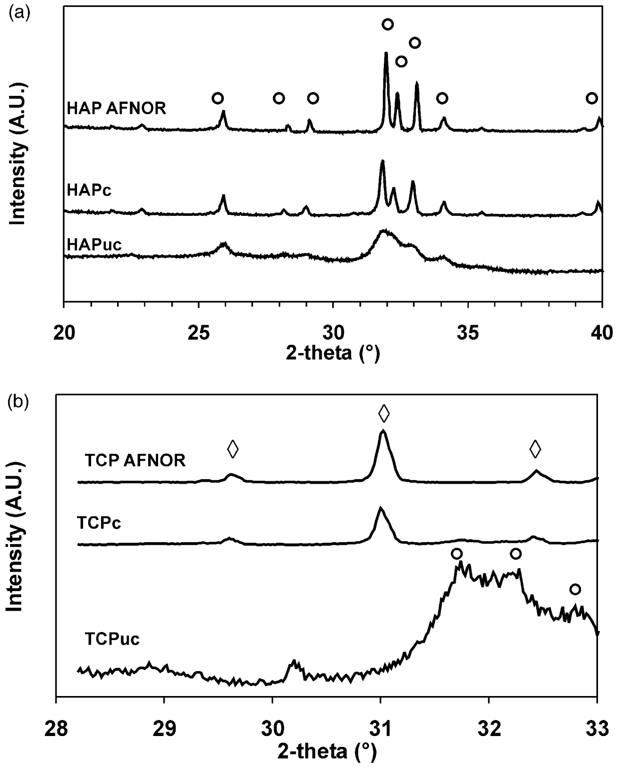

Fig. 3. Diffractograms of (a) HAPuc, HAPc and HAP calcinated according to the AFNOR standard; (b) TCPuc, TCPc and TCP calcined according to the AFNOR standard.

According to the respective Ca/P ratio of the powders, it can be deduced that HAPuc has the chemical formula $Ca_{10}(PO_4)_6(OH)_2$ and TCPuc $Ca_9(PO_4)_5(HPO_4)OH$.

After calcination at 720 °C, no structural change was detected for HAP. For TCPc, the calcination led to the formation of β-TCP according to the reaction:

$$Ca_9(PO_4)_5(HPO_4)OH \rightarrow 3Ca_3(PO_4)_2 + H_2O$$

XRD patterns also indicated a higher crystallinity of materials purified by calcination than the one of materials purified by washing.

3.2. Physical characteristics of the granules

Fig. 4 shows the particle size distributions of the granules. The distributions are similar for HAPuc and HAPc, and for TCPuc and TCPc respectively. The mean diameters are slightly higher for the TCP-based materials (about 300 μm) than for the HAP-based

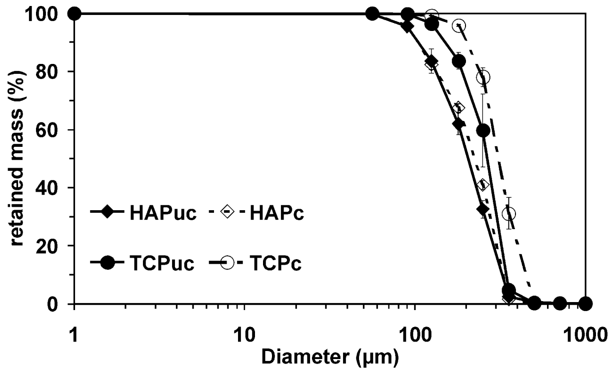

Fig. 4. Particle size distributions of the four materials.

materials (about 200 μm). The dispersion coefficients are close whatever the chemical nature (Table 2).

Table 2 shows the pycnometric densities of the four compounds under study. All the values were lower than the theoretical densities of hydroxyapatite (3.16 g cm^{-3}) and β-tricalcium phosphate (3.07 g cm^{-3}) due to the low crystallinity of the materials, even for calcined materials. Calcination increased the pycnometric density by enhancing the crystallinity of the materials. These results corroborate those obtained using X-ray diffraction showing patterns with broad peaks.

The bulk densities of the unpacked materials are shown in Table 2. The chemical nature of the materials highly influences this characteristic and the bulk densities of HAP are three times higher than those of TCP. This is due to differences in morphology of the granules: HAP granules are dense, whereas granules of TCP are looser and more porous. The morphology of the materials studied in SEM is shown in Fig. 5. The granules are constituted of elementary particles that are smaller for uncalcined powders than for calcined ones.

Calcination has no effect on the bulk density. It has been shown that high bulk densities are essential for direct compression excipients to incorporate important quantities of drug substance without losing their good compression properties.[17] From this point of view, the rather low bulk densities of TCP might be a disadvantage for its use in direct compression.

The specific surface areas are indicated in Table 2. Uncalcined materials exhibited high specific surface area (>40 m^{2}g^{-1}), whereas the thermal treatment dramatically decreased the surfaces (≈ 16 m^2 g^{-1}). From 400 to 750 °C, specific surface areas decrease due to a coalescence of the elementary particles without shrinkage. TCP-based materials show a higher decrease in the specific surface area due to a more important coalescence.

The powder porograms (Figs. 6) are different according to the chemical nature of the materials and the thermal treatment. Fig. 6a shows the pore size distributions of HAPuc and HAPc. Two classes are identified: the inter-granular pores with a mean pore diameter close to 30 μm and the intra-granular pores with a mean pore diameter of 0.04 μm. After calcination, the intra-granular pore distribution shifts to greater pore size due to a coalescence of the pores. This comes with a decrease in the specific surface area of the powders. The inter-granular porosity remains unchanged, justifying the unchanged values of the bulk densities. The total porosities determined from the programs are 71.2 and 74.0% for HAPuc and HAPc. Fig. 6b shows the pore size distributions of TCPuc and TCPc. The different classes of pores are less easy to identify. The pores have a large distribution, all over the range of studied pressures and the total porosities are higher than those of HAP, with values close to 80.6 and 87.6% for TCPuc and TCPc respectively. This is observed in SEM too with highly porous TCP granules.

Table 2
Physical properties of the materials

Compound	D_{50} (μm)[a]	Dispersion coefficient (μm)	d_{pycno}[a] (g cm^{-3})	d_{bulk}[a] (g cm^{-3})	Ss (m^{2}g^{-1})
HAPuc	210	130	2.89 (0.01)	0.65	44.55 (1.50)
HAPc	228	134	3.00 (0.00)	0.67	16.89 (0.31)
TCPuc	270	110	2.88 (0.02)	0.23	55.13 (0.41)
TCPc	310	127	3.01 (0.01)	0.17	11.84 (0.42)

[a] D_{50}: mean diameter; d_{pycno}: pycnometric density; d_{bulk}: bulk density.

3.3. Compression

The cycles of compression are plotted as pressure versus displacement (Fig. 7). The C_T values are 31 and 26%, respectively for HAPuc and HAPc, and 57 and 71%, for TCPuc and TCPc. These results express that HAP has a good packing ability whatever the thermal treatment. Previous works showed that HAP granules were rather spherical, that explains their ability to flow.[8] TCP is characterized by high C_T values. The total porosity (studied using mercury porosimetry) is higher for TCP than for HAP (83 versus 75%) and the pore distributions are much larger for TCP than for HAP (Figs. 6). The granules of TCP are highly porous and their morphology is irregular. All these characteristics are unfavorable to a good packing ability.

The Fig. 8 plots the NCW values versus the pressure of compaction. The global evolution is linear for all the materials. The initial values are the same for the four materials, for the lowest pressures of compaction (i.e. 10 MPa), and, they become twice higher for the two TCP materials than for the HAP, for higher pressures of compaction. A new interesting parameter has been developed to analyze the compression properties. This is the EW/NCW ratio which expresses the distribution of the total compression energy into elastic energy and net compression work, indicating the ability of the material to use the energy of compaction with a best yield. Fig. 9 shows the evolution of the EW/NCW ratio versus the pressure of compaction. For a same NCW value, the more important EW/NCW value, the more important the loss of energy into elasticity and, thus, the less effective the use of the energy for compaction. This ratio increases with the enhancement of the pressure of compaction: the higher the pressure of compaction, the more important the elastic work. The EW/NCW ratio is enhanced by calcination: the elastic work is more important for calcined materials than for uncalcined materials, whatever the chemical nature of the material. The ratio is slightly lower for TCP than for HAP, respectively for uncalcined and for calcined materials,

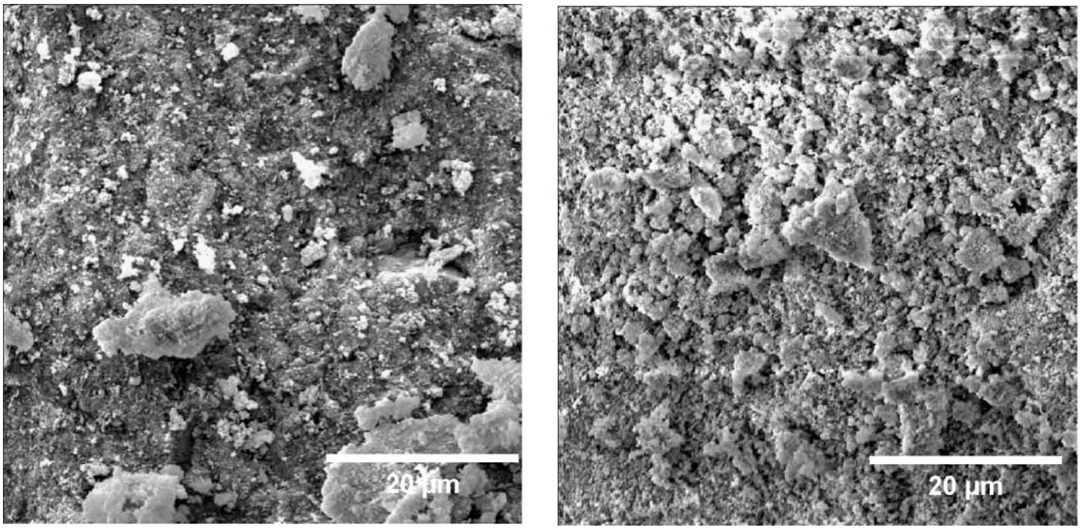

HAPuc (x1500) HAPc (x 1500)

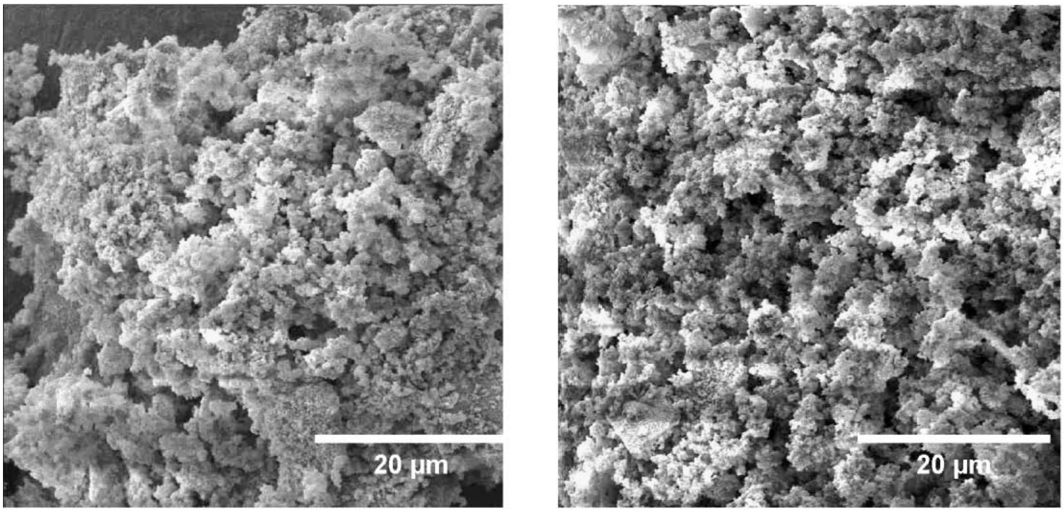

TCPuc (x1500) TCPc (x1500)

Fig. 5. Morphology of the powders (SEM).

but this difference is only significant for the highest pressures of compaction.

The Heckel plots were studied to determine the compression behavior of the four materials. The mean yield pressures are given in Table 3. All materials have Py values higher than 300 MPa characterizing highly-brittle materials. The chemical nature and the calcination do not seem to affect the degree of fragmentation of the materials.

The evolution of the compaction ratio versus the pressure of compaction is shown in Fig. 10. Both chemical nature and thermal treatment influence the evolution of the compaction ratio. The initial compaction ratio depends on the Ca/P molar ratio: it is lower than 10% for TCPuc and TCPc, and close to 20% for HAPuc and HAPc, due to the difference in the bulk densities. The final compaction ratios are lower for TCP than for HAP, with maximum values of 60% for TCPuc versus 65% for HAPuc.

The compression ranges of the four materials are shown in Table 3. The compression range of HAPuc is wide (10 to 250 MPa); beyond this pressure, lamination occurs. The compression range of the uncalcined TCP is larger and only limited by the press capacities: pressures from 10 to 300 MPa allow cohesive compacts without apparent lamination. The compression range is reduced from 100 to 150 MPa by calcination whatever the chemical nature. Different problems appear according to the nature of the material and explain this phenomenon: for pressures lower than 100 MPa, no breaking force can be measured for compacts of HAPc or TCPc, important sticking is also detected for TCPc linked to high elastic work and, for pressures higher than 150 MPa, compacts of HAPc and TCPc laminate.

3.4. Mechanical properties

Fig. 11 plots the evolution of the tensile strength versus the compaction ratio. Both chemical nature and thermal treatment influence the cohesion of the materials. On one hand TCP is the most cohesive material, this is more evident for uncalcined materials than for calcined ones. On the other hand, calcination induces a great decrease of the cohesion. TCPc and HAPc are 10 times less cohesive than TCPuc and HAPuc for a compaction ratio of 45%. This difference can be partially attributed to the difference in morphology and porosity between the granulated powders: the intra-granular porosity determined on the programs of the HAP-based materials (40%) is lower than the intra-granular porosity of TCP-based materials (55%), that might be a disadvantage for compaction.[18] In the case of calcined materials, the curves reach a limit tensile strength for compaction ratios lower than 50%, whereas tensile strength continues to increase for the highest compaction ratios for uncalcined materials, whatever the chemical nature. Previous works showed that calcination induces a decrease in cohesion due to a decrease of the specific surface of the powders. The evolution of the specific surface area is linked to a beginning of coalescence of the elementary particles.[8]

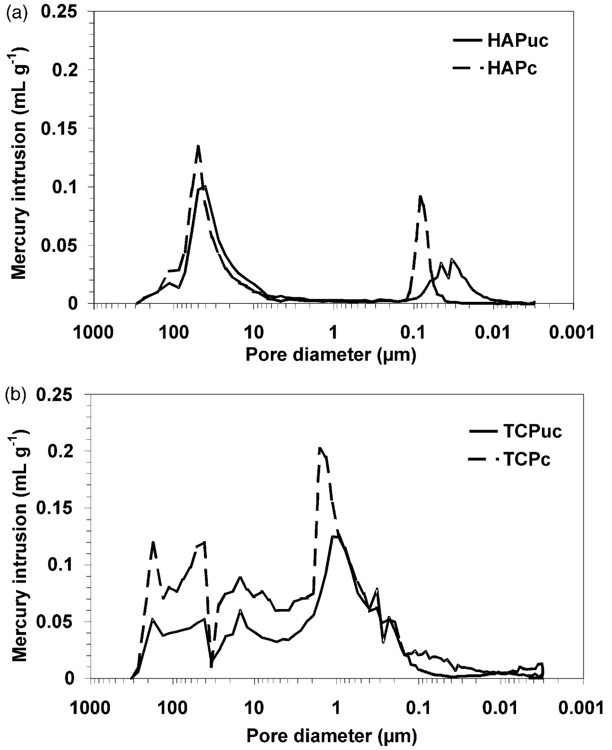

Fig. 6. Porograms of (a) HAPuc and HAPc; (b) TCPuc and TCPc.

Fig. 12 shows the evolution of the breaking work (*BW*) versus the net compression work (*NCW*). In several cases it was impossible to calculate the breaking work because of a lack of cohesion of the compact (for the low pressures) or because of cleavage (for the highest pressures). These problems were more common for the calcined materials that are, such a way, less easy-to-use than the uncalcined materials. It is obvious, according to this presentation, that the uncalcined materials are highly cohesive. The uncalcined apatitic tricalcium phosphate is the most cohesive material for one pressure of compaction as well as for one net compression work. This graph allows to determine the efficacy of compaction (C_{eff}) that is the slope of the linear regression.[19] The

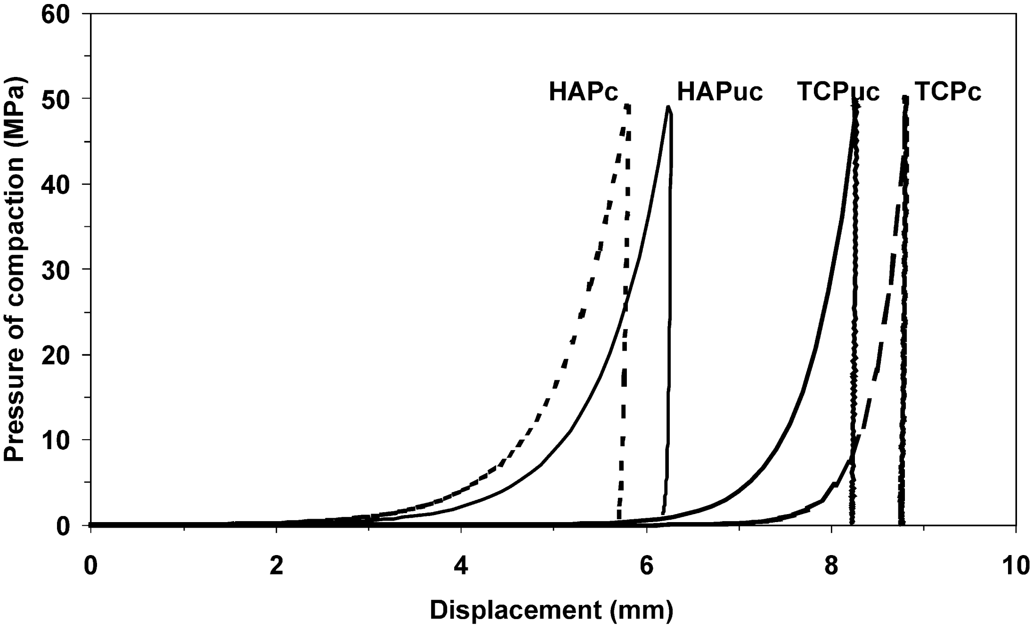

Fig. 7. Compression cycle of HAPuc, HAPc, TCPuc and TCPc for a compaction pressure of 50 MPa .

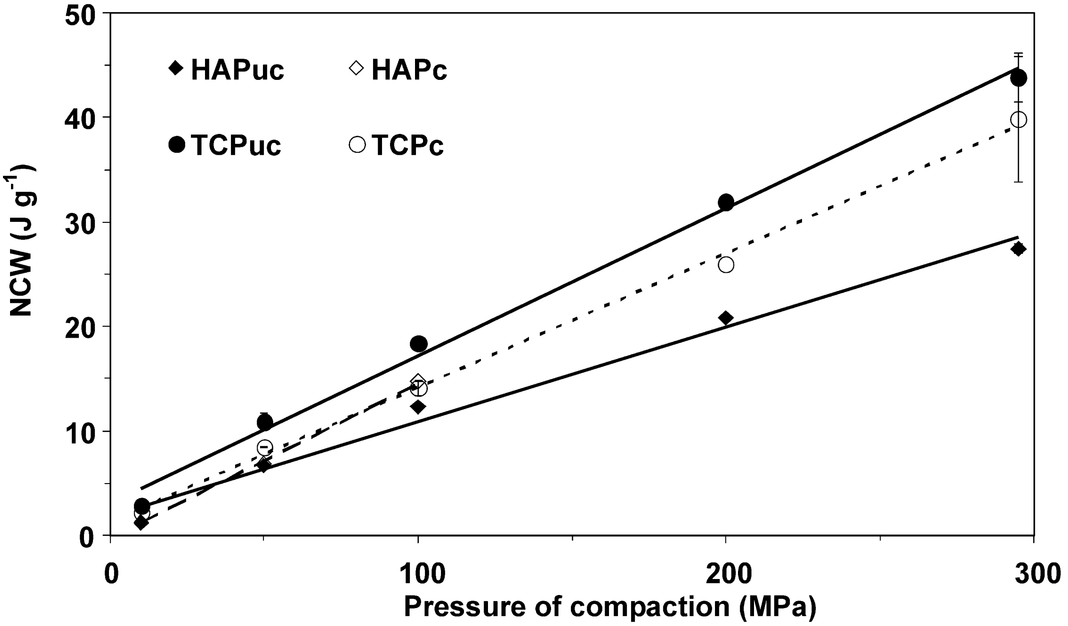

Fig. 8. Evolution of the net compression work of the four materials.

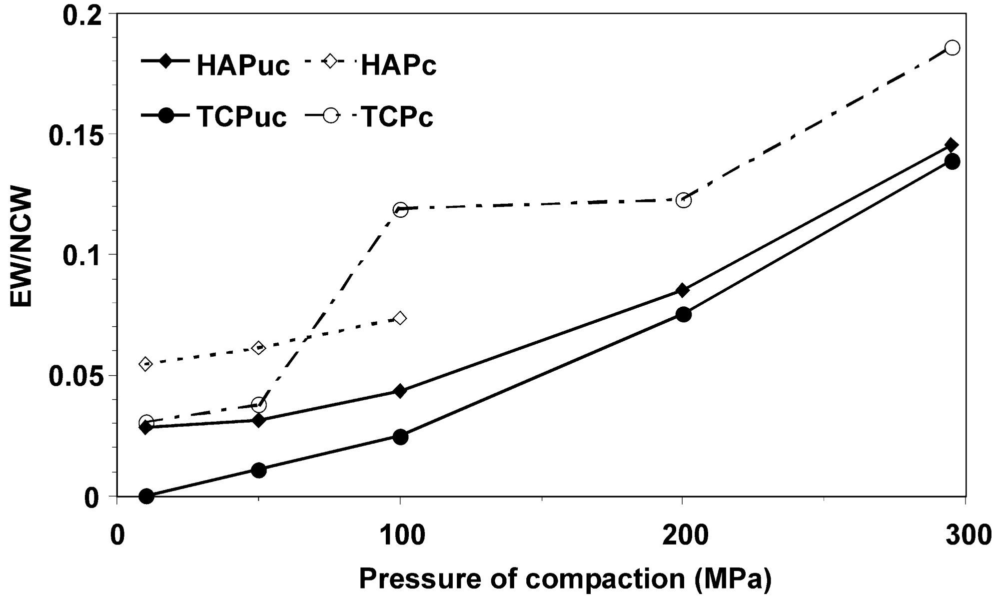

Fig. 9. Evolution of the *EW*/*NCW* ratio versus the pressure of compaction.

Table 3
Main parameters to choose the most outstanding material

	Flowability	Compaction properties			
	C_T (%)	Compression range (MPa)	*Py* (MPa)	R_d max (MPa)	Efficacy (× 10^{-4})
HAPuc	31	[10; 250]	357	2.6	3.0
HAPc	26	[100; 150]	500	0.2	2.0
TCPuc	57	[10; 295]	338	6.5	9.0
TCPc	71	[100; 150]	331	0.3	0.2

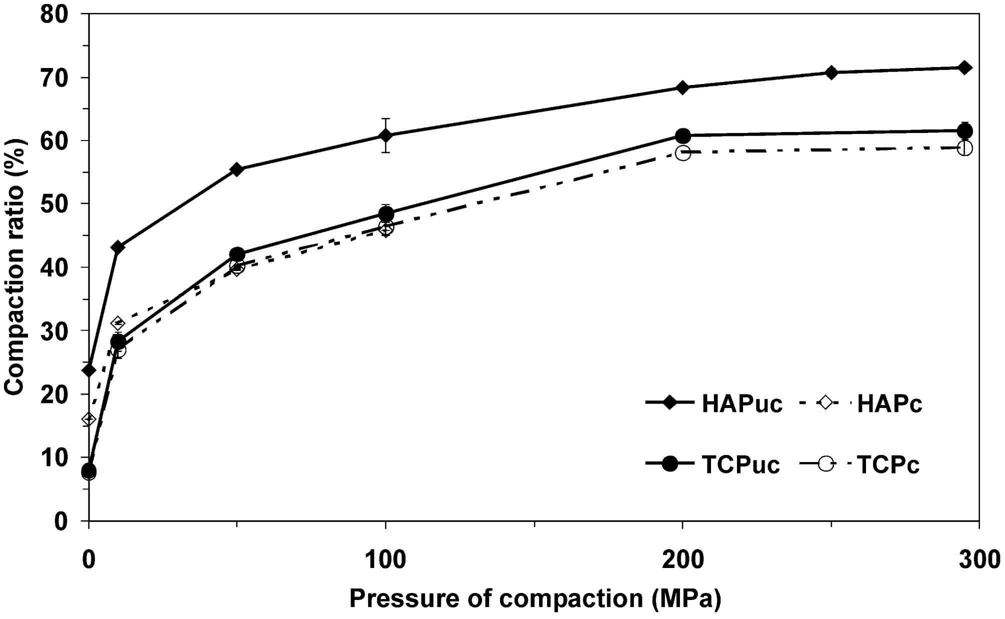

Fig. 10. Evolution of the compaction ratio as a function of the compaction pressure.

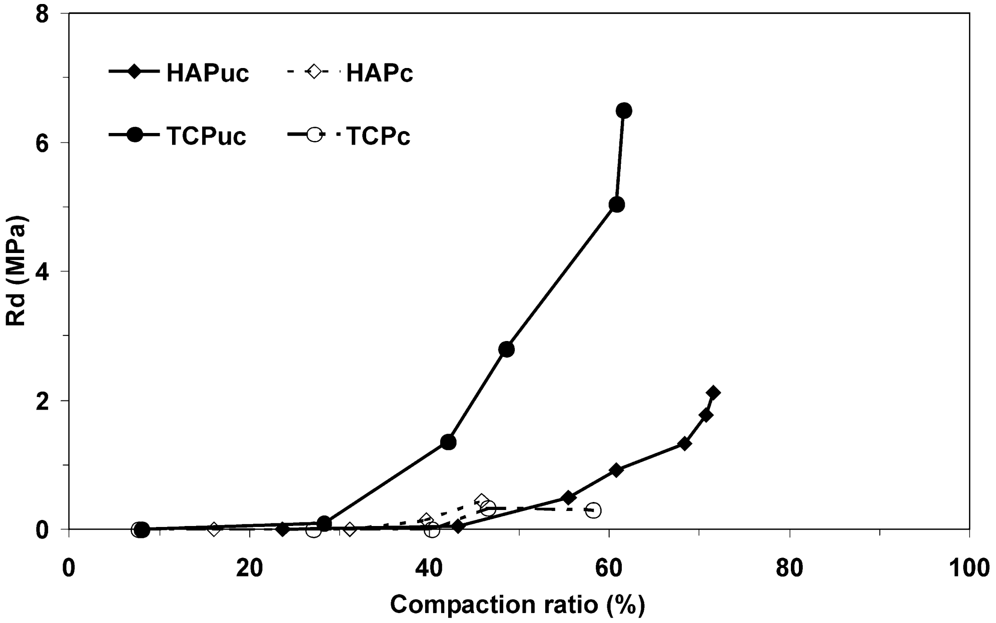

Fig. 11. Evolution of the tensile strength versus the compaction ratio.

efficacy of compaction is a useful new parameter allowing to study the compaction. It expresses the ability of the material to convert the compression work into cohesion. It gives more information than the measurement of the tensile strength which only indicates the degree of cohesion. C_{eff} indicates both the degree of cohesion (by means of the BW measurement), the use of the energy of compaction, and the eventual lamination. Previous works showed that slopes higher than 10.10^{-4} characterized a good efficacy of compaction.[19] The efficacy of compaction of TCPuc was the only one to be close to this limit (9.10^{-4}), making this compound usefull as a binder in direct compression. The C_{eff} value was $0.2.10^{-4}$ for TCPc, 3.10^{-4} and 2.10^{-4} for HAPuc and HAPc, respectively showing that these materials cannot be used for their binding properties. For TCPuc the *BW* versus *NCW* graph points out that lamination occurs for the highest pressures of compaction. There is a change in the slope of the curve corresponding to the lamination. This profile may be retained as a way to evaluate lamination.

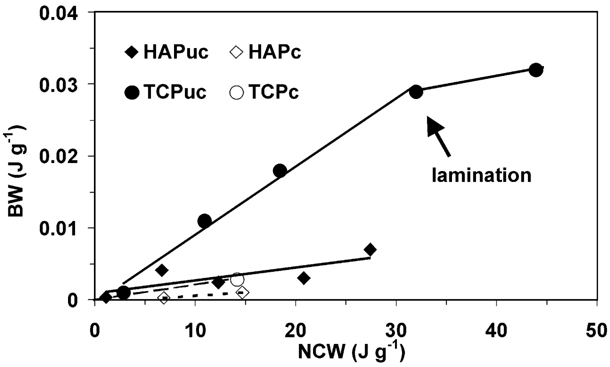

Fig. 12. Evolution of the breaking work versus the net compression work.

4. Conclusion

The calculation of the energies of compression allows to obtain several informations on the materials easily and with low quantities of product (less than 20 g for the whole mechanical study). It requires an instrumented press with an accurate extensometer and a force measuring sensor, and it can be carried out whatever the flow properties of the material (as mass flow is not required, on the contrary of the classically used compression machines). The results give information on the flowability of the powders in the compression cell by calculating the packing coefficient, using lower amounts of powder than traditional compaction characterization methods.[8] The compaction ratio is determined, and the calculation of the different energies during compaction allows to understand the consumption of the energy of compaction by the material. A new parameter (*EW*/*NCW* ratio) is proposed to apprehend the consumption of the energy during compression. The mechanical properties can easily be assessed and the calculation of the breaking energy gives more information than the classical tensile strength. It allows to calculate the efficacy of compaction defined as the ability of the material to convert the pressure of compaction into cohesion. This new and usefull parameter indicates how the material uses the energy to compact and the eventual existence of lamination.

This study was performed using four materials which are similar in chemical composition. That shows the sensitivity of the method. Table 3 summarizes the main parameters allowing to determine which material is the most interesting as direct compression excipient in pharmaceutical applications. Important differences were pointed out concerning the flowability: HAP had a better flowability than TCP. TCP will have to be associated to lubricants or to be particularly manufactured to be used in compression. The *EW*/*NCW* ratio indicated that the elasticity is more important in the case of the calcined materials.

Calculation of the efficacy of compression allows to discriminate the different materials. It showed that the apatitic tricalcium phosphate was the best studied material with a high densification during compression and a high cohesion, even for the lowest pressures of compaction. Its wide compression range makes it easy-to-use, and its good ability to use the energy of compaction makes it a good binder in pharmaceutical compression. Uncalcined hydroxyapatite is characterized by a large compression range, but a bad efficacy of compaction: it will not be used as a binder, but eventually as a filler in compression. Calcined materials, whatever their chemical nature, have a compression efficacy close to zero. Calcination alters the compression qualities due to a modification of the elementary particles constituting the granules and makes the calcined materials bad pharmaceutical excipients.

Further works using a more important number of materials have established correlations between C_T and the Carr coefficient, and between C_T and the bulk density and will be presented in another paper.

References

1. Young, R. A. and Holcomb, D. W., Variability of hydroxyapatite preparations. *Calcif. Tissue Int*, 1982, **34**, 17–32.
2. Conflant, P., Barthélémy, C., Guyot-Hermann, A. M., Guyot, J. C. and Semmoud, A., What is behind the marketed "tricalcium phosphate"? *S.T.P. Pharma*, 1997, **7**(4), 282–288.
3. Royer, A., Viguie, J. C., Heughebaert, M. and Heughebaert, J. C., Stoichiometry of hydroxyapatite: influence on the flexural strength. *J. Mater. Sci.: Mater. Med.*, 1993, **4**, 76–82.
4. Kohri, M., Miki, K., Waite, D. E., Nakajima, H. and Okabe, T., In vitro stability of biphasic calcium phosphate ceramics. *Biomater.*, 1993, **14**(4), 299–304.
5. Ducheyne, P., Radin, S. and King, L., The effect of calcium phosphate ceramic composition and structure on in vitro behavior. I. Dissolution. *J. Biomed. Mater. Res.*, 1993, **27**, 25–34.
6. Gauthier, O., Bouler, J. M., Aguado, E., Legeros, R. Z., Pilet, P. and Daculsi, G., Elaboration conditions influence physicochemical properties and in vivo bioactivity of macroporous biphasic calcium phosphate ceramics. *J. Mater. Sci.: Mater. Med.*, 1999, **10**, 199–204.
7. Gomez-Amoza, J. L. and Stanley-Wood, N. G., Relationships between flow properties, compression behavior and mechanical characteristics of prednisone-microcrystalline cellulose tablets. *Drug Dev. Ind. Pharm.*, 1991, **17**(9), 1241–1254.
8. Pontier, C., Viana, M., Champion, E., Bernache-Assollant, D. and Chulia, D., About the use of stoichiometric hydroxyapatite in compression—incidence of manufacturing process on compressibility. *Eur. J. Pharm. Biopharm.*, 2001, **51**(3), 249–257.
9. Matériaux pour implants chirurgicaux, Détermination quantitative du rapport Ca/P de phosphates de calcium, NF S-94-066, AFNOR, Paris, France, 1998.
10. Raynaud, S., Champion, E., Bernache-Assollant, D. and Laval, J. P., Determination of calcium/phosphorus atomic ratio of calcium phosphate apatites using X-ray diffractometry. *J. Am. Ceram. Soc.*, 2001, **84**(2), 359–366.
11. *European Pharmacopeia,* 3rd edn. Editions du Conseil de l'Europe, Strasbourg, France, 1997.
12. Vachon, M. G. and Chulia, D., The use of energy indices in estimating powder compaction functionality of mixtures in pharmaceutical tableting. *Int. J. Pharm.*, 1999, **177**, 183–200.

13. Gabaude, M. D., Gautier, J. C., Saudemon, Ph. and Chulia, D., Validation of a new pertinent packing coefficient to estimate flow properties of pharmaceutical powders at a very early development stage, by comparison with mercury intrusion and classical flowability methods. *J. Mater. Sci.*, 2001, **36**, 1–11.
14. Carr, R. L., Classifying flow properties of solids. *Chem. Eng.*, 1965, **72**(3), 69–72.
15. Heckel, R. W., Density-pressure relationships in powder compaction. *Trans. Metall. Soc. AIME*, 1962, **221**, 671–675.
16. Fell, J. T. and Newton, J. M., Determination of tablet strength by the diametral-compression test. *J. Pharm. Sci.*, 1970, **59**(5), 688–691.
17. Bolhuis, G. K. and Lerk, C. F., Comparative evaluation of excipients for direct compression, I. *Pharmaceutisch Weekblad*, 1973, **108**, 469–481.
18. Thomas, G., Structure and texture of solids. In: *Powder Technology and Pharmaceutical Processes*, ed. D. Chulia, M. Deleuil and Y. Pourcelot. Amsterdam, 1994.
19. Gabaude, C. M. D., Guillot, M., Gautier, J. C., Saudemon, Ph. and Chulia, D., Effects of true density, compacted mass, compression speed, and punch deformation on the mean yield pressure. *J. Pharm. Sci.*, 1999, **7**, 725–730.